

INFLUENCE OF DESIGN VARIABLES ON RADIATION HARDNESS OF SILICON

MINP SOLAR CELLS*

W. A. Anderson, S. Solaun, B. B. Rao, and S. Banerjee
State University of New York at Buffalo
Buffalo, New York

Metal-insulator-N/P silicon (MINP) solar cells were fabricated using different substrate resistivity values, different N-layer designs, and different I-layer designs. A shallow junction into an $0.3 \Omega\text{-cm}$ substrate gave best efficiency whereas a deeper junction into a $1\text{-}4 \Omega\text{-cm}$ substrate gave improved radiation hardness. I-layer design variation did little to influence radiation hardness.

INTRODUCTION

Recent trends in silicon solar cell research point towards increased efficiency. Shallow junction N/P solar cells have been reported with efficiency in the 16 - 18% range (ref. 1,2). The MINP solar cell was introduced by M. A. Green because of the high open circuit voltage. This type of cell utilizes an insulator layer over the shallow N^+ region followed by a low work function metal grid. This combination reduces surface recombination and dark current, while providing an electric field to increase ultraviolet response and efficiency.

Solar cells for extraterrestrial applications must withstand electron, proton, and U.V. radiation while being designed for high efficiency and light weight. Many aspects of space radiation effects and solar cell performance are discussed in the Solar Cell Radiation Handbook published by Jet Propulsion Laboratory and NASA (ref. 3). A preliminary report on MINP solar cells was published in IEEE Transactions on electron Devices (ref. 4). The work reported herein is an extension of the preliminary work in considering different MINP solar cell designs and the resultant influence of 1.0 MeV electron irradiation.

THEORETICAL CONSIDERATIONS

On a theoretical basis, high efficiency cells should have a shallow junction depth (x_j) to minimize recombination of photo-generated carriers, high emitter doping (N_D) to give a favorable electric field profile, and base doping (N_A) of about $7 \times 10^{17}/\text{cm}^3$ to give a low value of reverse saturation current (J_{ob}) while preserving a large diffusion length (L_n). These requirements are illustrated by using several rather fundamental equations. The basic dark current density equation is

* The work described in this paper was performed in part under the sponsorship and technical direction of International Telecommunications Satellite Organization (INTELSAT). Any views expressed are not necessarily those of INTELSAT.

$$J = (J_{oe} + J_{ob}) (e^{qV/kT} - 1) + J_{or} (e^{qV/2kT} - 1) \quad (1)$$

$$\text{where } J_{ob} = \frac{qn_i^2 D_n}{N_A L_n} \quad (2)$$

$$J_{oe} \approx \frac{qn_i^2 S_p}{N_D} \ll J_{ob} \quad (3)$$

$$J_{or} = \frac{qn_i x'}{\tau_0} \ll J_{ob} \quad (4)$$

In these equations J_{ob} = base current contribution, J_{oe} = emitter current contribution, J_{or} = space charge layer recombination current contribution, N_A = substrate doping density, L_n = diffusion length in the substrate, S_p = surface recombination velocity, N_D = doping in the emitter assuming a uniform doping profile, x' = space charge layer width, and τ_0 = carrier lifetime. The other terms have their usual meaning. Open circuit voltage may also be calculated using

$$V_{oc} = \frac{nkT}{q} \ln \left(\frac{J_{sc}}{J_0} \right) \quad (5)$$

If $J_{ob} > J_{oe}$ for substrate control, then

$$V_{oc} = \frac{nkT}{q} \ln \left(\frac{J_{sc} N_A L_n}{qn_i^2 D_n} \right) \quad (6)$$

and with $J_{oe} > J_{ob}$ for emitter control,

$$V_{oc} = \frac{nkT}{q} \ln \left(\frac{J_{sc} N_D}{qn_i^2 S_p} \right) \quad (7)$$

Equations 3 and 7 clearly show the importance of low surface recombination velocity (S_p) which is achieved in MINP and MNP-P cells by oxide passivation.

EXPERIMENTAL METHODS

The ion-implanted cells were fabricated by implanting ^{31}P at 5 KeV, $2.5 \times 10^{15}/\text{cm}^2$ onto 0.3 $\Omega\text{-cm}$ p-type silicon substrates. The samples were annealed at 850 $^\circ\text{C}$ (30 minutes, N_2 flow) followed by 550 $^\circ\text{C}$ for 1 hour to remove the implantation damage. The back ohmic contact was formed by thermally evaporating Al which was sintered at 500 - 600 $^\circ\text{C}$ during which time a thin oxide layer was allowed to grow over the entire n-surface for the fabrication of MINP solar cells. Ytterbium, a low work function metal, followed by Cr and Al, was used for the grid contact.

Thermally evaporated SiO_x served as the antireflection coating. In the case of the MNP-P solar cell, a thick ($\approx 300 \text{ \AA}$) SiO_2 layer was grown over the entire n-surface. Photolithography techniques were used to remove the oxide in regions where the grid contact was to be formed. Examples of these cells are given in Figure 1.

Several values of implantation energy and substrate resistivity were chosen to examine the theoretical predictions and evaluate radiation effects as well which may not have an obvious result. Thus, implant energies of 5, 10 and 30 kV were used with substrate resistivities of 0.1-0.3, 0.3 and 1-4 $\Omega\text{-cm}$ as shown in Table I. Also, some MNP-P cells were fabricated by bubbling O_2 through trichloroethylene (TCE) (ref. 5) which produces a Cl-containing oxide for improved surface passivation. This should reduce S_p to improve photovoltaic response as predicted by equations 3 and 7.

Completed cells were tested for photovoltaic performance and spectral response after edge isolation by a diamond saw. An ELH quartz halogen lamp was calibrated for AMO illumination by a p/n junction cell previously tested at the NASA-Lewis Research Center. Spectral response was measured using a Schoeffel GM-100 monochromator from $0.4 \mu\text{m}$ - $1.0 \mu\text{m}$. Samples were irradiated at 1.0 MeV using a Model GS High Voltage Engineering Van de Graff accelerator with a water cooled stage to prevent thermal damage during irradiation. Samples were irradiated at fluence levels of $1.0 \times 10^{14}/\text{cm}^2$, $1.0 \times 10^{15}/\text{cm}^2$ and $1.0 \times 10^{16}/\text{cm}^2$ after which the previously mentioned measurements were conducted.

EXPERIMENTAL DATA

Resistivity and Implant Energy

Two MINP solar cells were fabricated from each of four pairs of the design variables, substrate resistivity (ρ_s) and implant energy (E). These four conditions are clearly listed in Tables I and II. Table I considers diode factor and reverse saturation current density from dark and illuminated I-V curves. Lower n-values and J_0 -values are seen when using lower values of ρ_s as predicted by eq. (2). A lower implant energy is also advantageous since lattice damage is reduced and a sharper electric field profile exists to reduce carrier recombination. Spectral response at $\lambda = 0.4 \mu\text{m}$ is improved for shallow junctions since collection of U.V. photons would be more efficient.

Radiation effects on the subject samples are listed in Table II indicating a greater stability for higher ρ_s . This is not surprising since less dopant reduces radiation interaction with the dopant atom to create fewer recombination centers.

MINP vs MNP-P-0 vs MNP-P-T

Cells with a $\approx 22 \text{ \AA}$ I-layer over the entire surface (MINP) were compared with those having a $\approx 150 \text{ \AA}$ standard SiO_2 I-layer between grid lines (MNP-P-0) or those having a $\approx 150 \text{ \AA}$ Cl-containing SiO_2 I-layer between grid lines (MNP-P-T). Table I indicates reduced values of n-factor and J_0 for the MNP-P variety since tunneling

through the thin I-layer is eliminated. A statistical comparison of photovoltaic (PV) data for the three kinds of cells, in Table III, indicates the MINP cell to be more efficient due to increased J_{sc} and V_{oc} . This is attributed to perhaps less optical absorption in the I-layer and to reduced recombination under the grid lines in MINP cells. The MNP-P-T cells are slightly more efficient than the MNP-P-0 variety which we attribute to reduced surface recombination from Cl in the oxide.

Spectral response data of Figure 2 indicate the relative order of superiority from MINP to MNP-P-T to MNP-P-0 which agrees with data in Table III. Effects of 1.0 MeV irradiation, shown in Table IV, do not indicate a significant difference on radiation hardness between these 3 kinds of cells. This points to the substrate as the main point of degradation whereas the surface damage is minimal.

Effects of irradiation on dark I-V data for MINP compared to MNP-P-T cells is given in Figures 3 and 4. At low voltages, MINP cells exhibit an increased current component, which may be due to tunneling and which is quite insensitive to irradiation. The MNP-P-T cell current was sensitive to radiation at low voltages and more sensitive at higher voltages than was the MINP cell. Irradiation effects on spectral response were quite similar for all 3 designs with an example given for the MNP-P-T cell in Figure 5. All cells exhibited a trend towards increased U.V. response after $10^{16} e^-/cm^2$ irradiation which at this time is unexplained. The trend was most prevalent for the pictured MNP-P-T variety.

DISCUSSION

MINP-type cells are quite insensitive to 1.0 MeV e^- irradiation in the U.V. response meaning that the surface damage is minimal. Most reduction in performance is due to bulk damage as evidenced by spectral response data, increased J_o , decreased V_{oc} , and decreased J_{sc} . Diffusion length typically decreases to 8-10 μm at $10^{16} e^-/cm^2$ regardless of the starting value. There is a trend in cell efficiency to decrease to a certain value even though original efficiency values may vary. The measured value of L_n in equation (2) accurately predicts the increased J_{ob} which accurately predicts the reduced V_{oc} using equation (5). For example, equation (2) predicts $J_{ob} = 3 \times 10^{-13} A/cm^2$ before irradiation with $L_n = 250 \mu m$ and $1.2 \times 10^{-11} A/cm^2$ after irradiation with $L_n = 6 \mu m$. This corresponds to a change in V_{oc} from 669 mV to 554 mV which is 115 mV or 17% whereas experimentally we observed an average change of about 105 mV which is 17%. The good agreement between experiment and theory is evidence that bulk damage and not surface damage is the controlling factor in degradation. MINP cell efficiency is maximized for $\rho_s = 0.3 \Omega\text{-cm}$ whereas the radiation tolerance is improved for $\rho_s > 1.0 \Omega\text{-cm}$. A design trade-off is thus suggested to obtain both high efficiency and radiation hardness. Figure 6 gives a comparison of V_{oc} and efficiency loss due to irradiation for the MINP cell, conventional, and advanced N/P Si cells. The MINP cell is clearly superior in V_{oc} and in efficiency for electron fluence $< 10^{15} e^-/cm^2$. The proposed new goals for surface passivated cells would predict a performance superior to existing silicon cells. Use of Ga-doped Si (ref. 6) or Li counterdoping (ref. 7) may give an MINP cell with even better performance at high fluence levels.

REFERENCES

1. Young, R. T.; Van der Leeden, G. A.; Sanstrom, R. L.; Wood, R. F.; and Westbrook, R. D.; "High Efficiency Si Solar Cells by Beam Processing," Appl. Phys. Lett., 43, pp. 666-668, 1983.
2. Blakers, A. W.; Green, M. A.; Jiquan, S.; Keller, E. M.; Wenham, S. R.; Godfrey, R. B.; Szpitalak, T.; and Willison, M. R.; "18 - Percent Efficient Terrestrial Silicon Solar Cells," IEEE Electron Device Letters, EDL-5, pp. 12-14, January 1984.
3. Tada, H. Y.; Carter, Jr., J. R.; Anspaugh, B. E.; and Downing, R. G.; Solar Cell Radiation Handbook, Third Edition, JPL Publication, 82-69, 1982.
4. Thayer, M.; Anderson, W. A.; and Rao, B. B.; "Reliability of MINP Compared to MIS, SIS and N/P Silicon Solar Cells Under 1.0 MeV Electron and Environmental Effects," IEEE Trans. on Elec. Dev., ED-31, pp. 619-621, May 1984.
5. Jackson, M. A.; Rao, B. B.; and Anderson, W. A.; "Improved Performance of Surface-Passivated Solar Cells by Chlorine-Containing Oxides," J. Appl. Phys., to appear May 15, 1985.
6. Minahan, J. A.; and Trumble, T. M.; "Electron Irradiated Solar Cells: Cold Crucible (Ga), Float Zone (Ga, B), and Czochralski (Ga, B), Proc. 17th IEEE Photovoltaic Specialists Conference, Orlando, p. 144, 1984.
7. Weinburg, J.; Mehta, S.; and Swartz, C. K.; "Radiation Damage and Defect Behavior in Ion-Implanted Lithium Counterdoped Silicon Solar Cells," Proc. 17th IEEE Photovoltaic Specialists Conference, Orlando, p. 1088, 1984.

TABLE I

INFLUENCE OF FABRICATION CONDITION ON COMPONENTS OF I-V EQUATION

Substrate Resistivity (Ω -cm)	Implant Energy (kV)	Diode Factor		Reverse Saturation Current Density		Spectral Response @ 0.4 μ m (mA/mW)
		Dark n_d	Light n_l	J_{od} (mA/cm ²)	J_{ol} (mA/cm ²)	
1 - 4	30	1.69	1.28	4.5×10^{-8}	2.5×10^{-9}	0.19
0.1 - 0.3	30	1.80	1.33	1.8×10^{-7}	2.0×10^{-9}	0.20
0.3	10	1.58	1.15	3.0×10^{-9}	4.0×10^{-11}	0.22
0.3	5	1.58	1.17	4.0×10^{-9}	5.0×10^{-11}	0.24
0.3	5 [*]	1.42	1.05	1.2×10^{-9}	9.8×10^{-12}	
0.3	5 ^{**}	1.39	1.05	7.9×10^{-10}	8.0×10^{-12}	

* MNP-P-O

** MNP-P-T

TABLE II

EFFECT OF 1.0 MeV e^- RADIATION UPON AVERAGE PHOTOVOLTAIC OUTPUT OF MINP CELLS HAVING DIFFERENT SUBSTRATE RESISTIVITY AND IMPLANTATION ENERGY*

OPEN CIRCUIT VOLTAGE, V_{oc}

Cell Numbers	Substrate Resistivity (Ω -cm)	Implant Energy (kV)	Initial Value (V)	After $10^{15} e^-/cm^2$		After $10^{16} e^-/cm^2$	
				(V)	(% dec.)	(V)	(% dec.)
694, 697	1 - 4	30	0.575	0.527	8.4	0.490	14.6
714, 716	0.1 - 0.3	30	0.585	0.556	4.9	0.516	11.9
745, 746	0.3	10	0.600	0.563	6.2	0.516	14.0
776, 784	0.3	5	0.618	0.569	7.9	0.516	16.5

SHORT CIRCUIT CURRENT DENSITY, J_{sc}

Cell Numbers	Substrate Resistivity (Ω -cm)	Implant Energy (kV)	Initial Value (mA/cm^2)	After $10^{15} e^-/cm^2$		After $10^{16} e^-/cm^2$	
				(mA/cm^2)	(% dec.)	(mA/cm^2)	(% dec.)
694, 697	1 - 4	30	46.2	36.0	22.0	28.6	38.2
714, 716	0.1 - 0.3	30	42.2	30.6	27.4	20.7	51.0
745, 746	0.3	10	42.7	30.5	28.6	21.5	44.6
776, 784	0.3	5	45.7	34.0	25.6	23.4	48.0

EFFICIENCY, η

Cell Numbers	Substrate Resistivity (Ω -cm)	Implant Energy (kV)	Initial Value (%)	After $10^{15} e^-/cm^2$		After $10^{16} e^-/cm^2$	
				(%)	(% dec.)	(%)	(% dec.)
694, 697	1 - 4	30	13.5	9.3	30.9	7.1	47.6
714, 716	0.1 - 0.3	30	12.5	8.2	34.2	5.2	57.6
745, 746	0.3	10	14.2	9.4	34.2	5.0	64.3
776, 784	0.3	5	15.6	9.9	36.6	4.8	69.2

* Simulated AMO illumination. All J_{sc} and η -values are based on active area. Total area is about 10% more.

TABLE III
 STATISTICAL DATA FOR PHOTOVOLTAIC PERFORMANCE OF
 MINP, MNP-P-0 AND MNP-P-T SOLAR CELLS*

Cell #	V_{oc} (mV)	J_{sc} (mA/cm ²)	FF	η (%)	Type of Cell
737	630	35.1	0.70	15.5	MINP
703	617	36.9	0.72	16.4	MINP
765	631	36.7	0.80	18.5	MINP
769	626	35.1	0.80	17.5	MINP
730	624	35.9	0.72	16.2	MINP
784	615	35.1	0.77	16.6	MINP
Average	624	35.8	0.75	16.8	
Standard Deviation	6.04	0.76	0.04	0.97	
720	610	34.8	0.74	15.8	MNP-P-0
735	624	34.5	0.74	16.0	MNP-P-0
731	611	32.1	0.73	14.4	MNP-P-0
Average	615	33.8	0.74	15.4	
Standard Deviation	6.38	1.21	0.005	0.71	
756	622	34.3	0.78	16.6	MNP-P-T
783	606	34.5	0.78	16.4	
750	615	31.8	0.74	14.5	
Average	614	33.5	0.77	15.8	
Standard Deviation	6.55	1.22	0.02	0.94	

* Tested with simulated AM1 illumination

TABLE IV

PHOTOVOLTAIC DATA COMPARING MNP-P-O, MNP-P-T, AND MINP

	Open Circuit Voltage			Short Circuit Current Density**			Efficiency**		
	Initial Value (mV)	Change (mV)	% Change (%)	Initial Value (mA/cm ²)	Change (mA/cm ²)	% Change (%)	Initial Value (%)	Change (%)	% Change (%)
735 ^a Rad 1*	632	37	5.8	47.0	6.6	14.0	16.3	3.0	18.4
Rad 2		72	11.4		13.5	29.0		6.1	37.4
Rad 3		120	19.0		22.6	48.1		9.9	60.8
782 ^a Rad 1	604	20	3.3	44.4	5.1	11.5	14.7	2.1	14.3
Rad 2		44	7.3		11.9	26.8		5.0	34.0
Rad 3		99	16.4		21.4	48.2		8.9	60.8
783 ^b Rad 1	608	15	2.5	46.7	5.1	10.9	16.4	2.5	15.2
Rad 2		43	7.1		12.1	25.9		5.7	34.8
Rad 3		97	16.0		22.1	47.3		10.0	60.9
756 ^b Rad 1	626	31	4.9	45.7	6.5	14.2	15.7	2.9	18.5
Rad 2		61	9.7		12.8	28.0		5.8	36.9
Rad 3		116	18.5		22.5	49.2		9.5	60.4
768 ^c Rad 1	602	22	3.6	48.2	7.4	15.4	15.5	2.9	18.7
Rad 2		52	8.6		14.4	29.9		6.0	38.7
Rad 3		98	16.3		24.3	50.4		9.4	60.8
785 ^c Rad 1	608	19	3.1	43.2	0.8	1.8	15.0	1.1	7.3
Rad 2		51	8.4		8.6	19.9		4.7	31.3
Rad 3		102	16.8		18.0	41.7		8.6	57.2

* Rad 1 = 1×10^{14} e⁻/cm², Rad 2 = 1×10^{15} e⁻/cm², Rad 3 = 1×10^{16} e⁻/cm².

** Tested at simulated AMO using a GE-ELH lamp.

(a) MNP-P-O, (b) MNP-P-T, (c) MINP

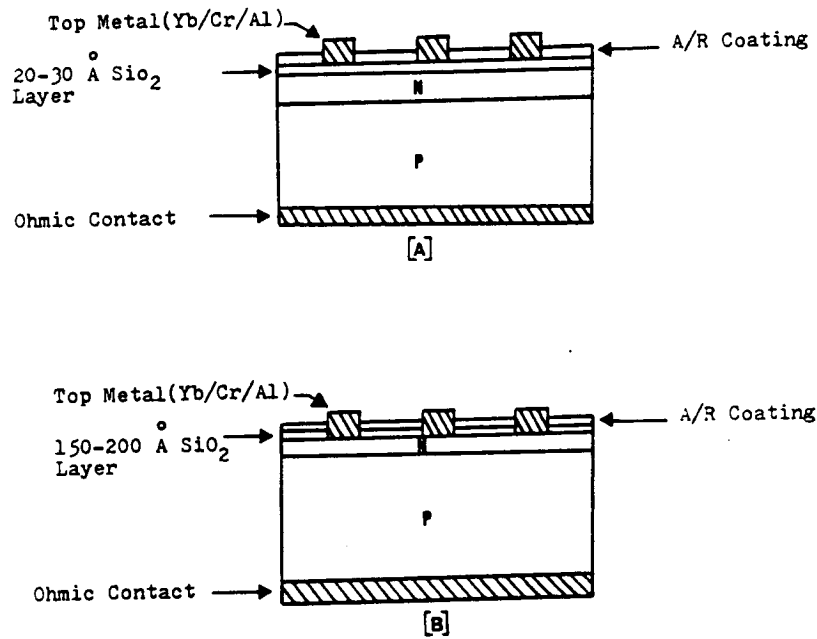


Figure 1: Diagram of [A] MINP and [B] MNP-P cells.

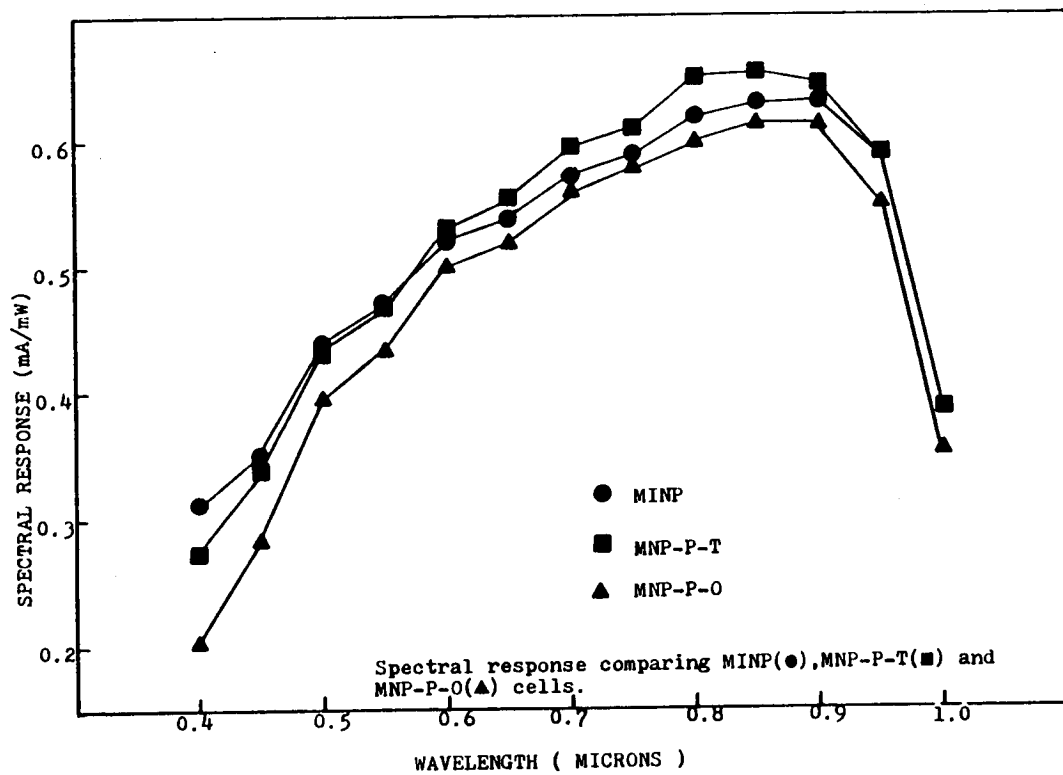


Figure 2: Spectral response of MINP, MNP-P-O, and MNP-P-T cells.

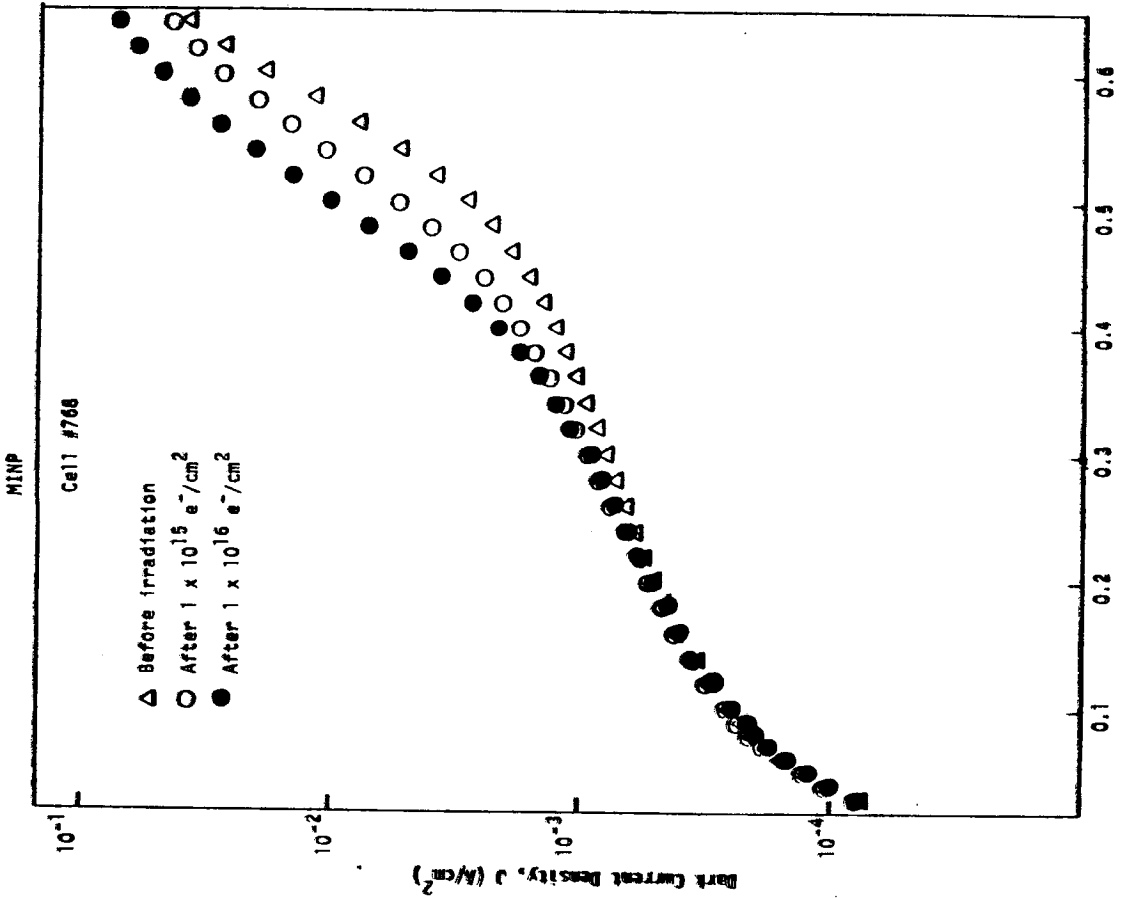


Figure 3: Dark J-V for a MINP cell as a function of e^- irradiation.

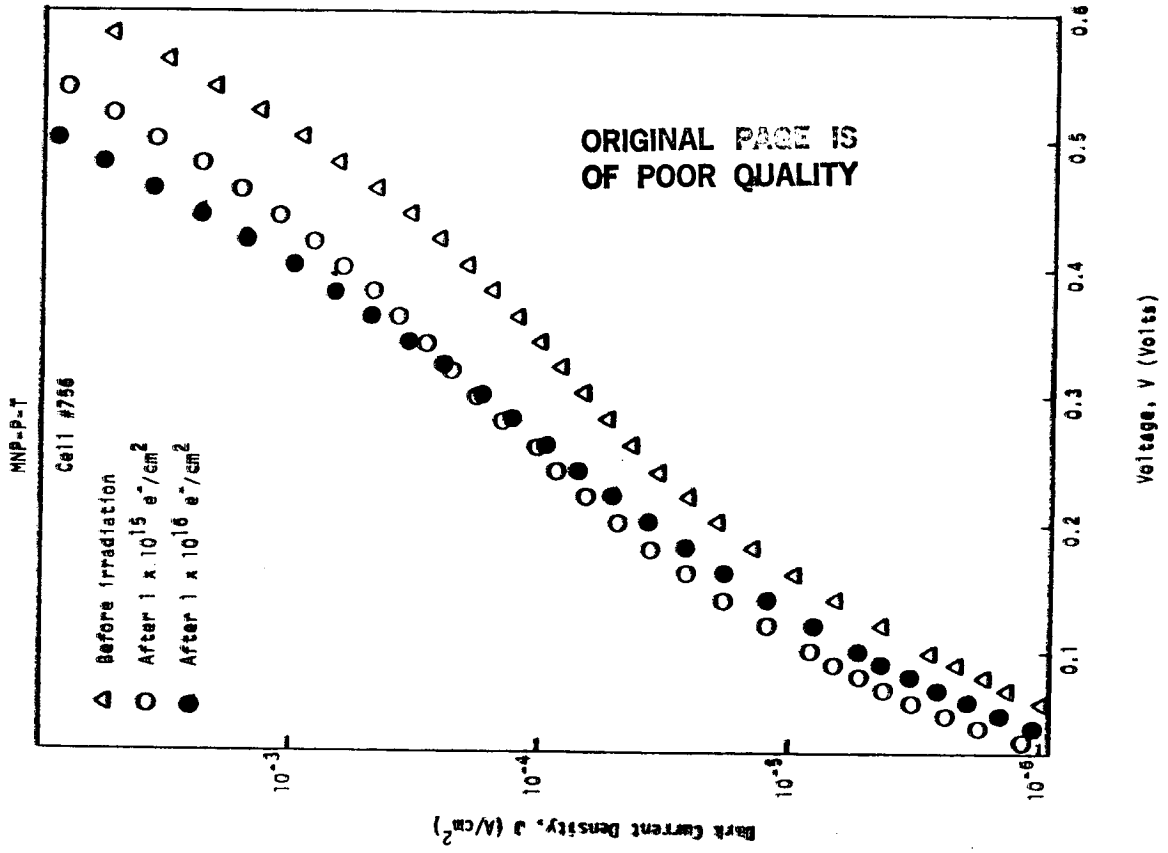


Figure 4: Dark J-V for a MNP-P-T cell as a function of e^- irradiation.

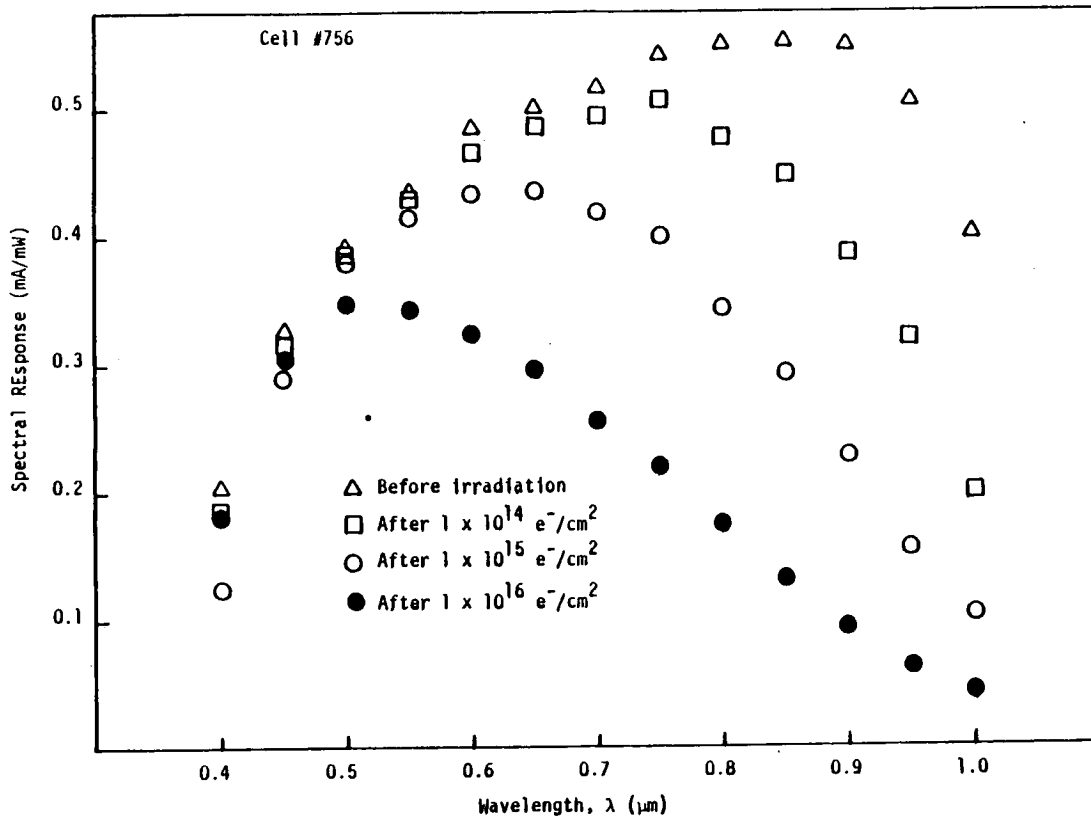


Figure 5: Spectral response of a MNP-P-T cell as a function of e^- irradiation.

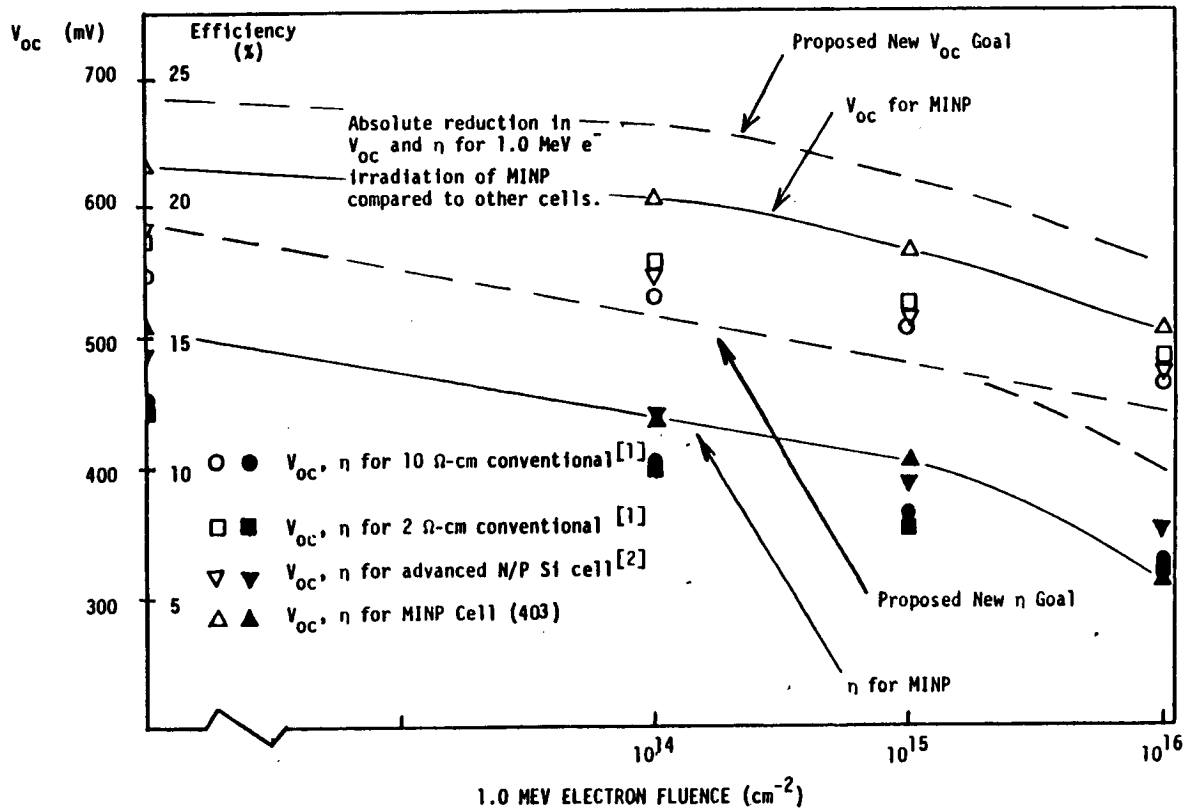


Figure 6: Photovoltaic data variation with e^- fluence for several cells.